

The 4th International Conference on Sustainable Energy Information Technology (SEIT-2014)

Modeling Weather Impact on a Secondary Electrical Grid

Dingquan Wang^a, Rebecca J. Passonneau^{a,*}, Michael Collins^a, Cynthia Rudin^b

^aColumbia University, New York, NY 10027, USA

^bMassachusetts Institute of Technology, Cambridge, MA 02139, USA

Abstract

Weather can cause problems for underground electrical grids by increasing the probability of serious “manhole events” such as fires and explosions. In this work, we compare a model that incorporates weather features associated with the dates of serious events into a single logistic regression, with a more complex approach that has three interdependent log linear models for weather, baseline manhole vulnerability, and vulnerability of manholes to weather. The latter approach more naturally incorporates the dependencies between the weather, structure properties, and structure vulnerability.

© 2014 The Authors. Published by Elsevier B.V.

Selection and peer-review under responsibility of Elhadi M. Shakshuki.

Keywords: Secondary Electrical Grid; Machine Learning; Expectation-Maximization; Log-Linear Model; Semantic Dependency; Interpretable Models

1. Introduction

Every major power grid contains a “secondary” network that delivers power directly to customers. Since 2007, we have worked with the Consolidated Edison Company of New York to derive statistical models for predictive and causal analysis of events in the Manhattan secondary grid, which consists largely of underground electrical cables. The sustainability problem we address is how to leverage existing offline data to assess the causes of events that lead to major service interruptions. In previous work, we developed a process to integrate and extend raw unlabeled data from distinct business units at Con Edison, then to apply a supervised ranking algorithm¹ to rank nodes in the secondary grid, where these are manholes and service boxes, in terms of their vulnerability to serious events in the following year.² Over time, we have noticed that the predictive accuracy of our models varies from year to year, in part because of changes in Con Edison’s infrastructure and customer usage, but also very much due to changes in the severity of the weather. Our focus here is to design a model that incorporates the dependence of structure vulnerability on weather conditions that stress the secondary grid.

The Manhattan secondary grid consists of more than 40,000 underground electrical *structures* (manholes and service boxes) that distribute power through a highly redundant mesh grid of mains cables that connect the structures to each other, and service cables that connect customers (buildings) to the secondary grid. Our previous ranking models yield a probability of a serious event for each structure based on a representation of structures in terms of the number

* Corresponding author. Tel.: +1-212-870-1278 ; fax: +1-212-870-1285.

E-mail address: becky@ccls.columbia.edu

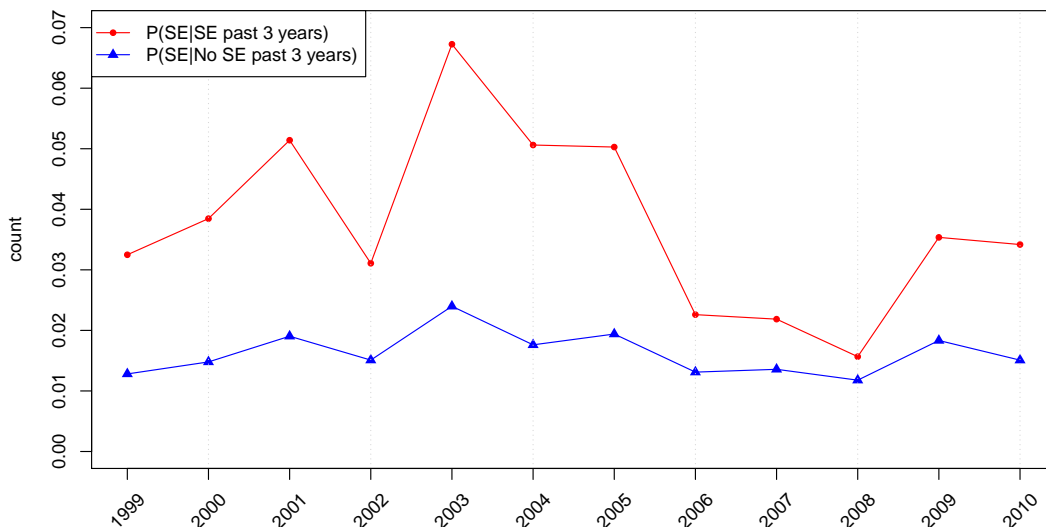


Fig. 1. The conditional probability of a serious event (SE), given a history of serious events in the past three years (red line), or not (blue line).

and makeup of the cables they house, and their past history of involvement in events, from low-grade to serious ones. A trouble ticket system documents events on the grid. Explosions and fires in structures are clearly serious events, and are also relatively rare. Flickering lights in a building constitute a non-serious event. A smoking manhole can be serious or non-serious. We have done considerable work to automatically identify a class of serious events based on information from trouble tickets and other databases,³ based on a study where expert engineers classified events.⁴

The inspiration for the current work can be explained by reference to Figure 1. The axes are time (x-axis) and rate of events (y-axis). The red line plots the probability that a structure will have a serious event, conditioned on whether the structure had a serious event in the previous three years ($P(SE|SE \text{ past } 3 \text{ years})$). The blue line represents the probability a structure will have an event, given no serious event in the previous three years ($P(SE|No SE \text{ past } 3 \text{ years})$). Because the red line is always above the blue line, prior history is a predictor of serious events. The ups and downs of the red line show that likelihood of serious events varies considerably from year to year, and more so for structures with a history of serious events. Con Edison engineers have observed that bad weather conditions, such as snowmelt combined with salt, increase the rate of serious events. What is not clear is exactly which weather factors are most stressful to the grid, and which features of underground structures make them more vulnerable to weather. Here we present a tri-partite model that captures the dependencies between weather features, structure features pertaining to their baseline vulnerability, and structure features that represent their enhanced vulnerability during bad weather.

2. Related Work

Machine learning (ML) techniques have been used to analyze power systems for over a decade.^{5,6} Our collaborators have applied ML to the problems of smart grid control,⁷ or preventive maintenance;⁸ other power problems addressed through ML include power management,⁹ and microgrids.¹⁰ ML has also been applied to the problem of predicting models for solar-power generation from weather data.¹¹ We believe the present paper is the first attempt to model the impact of weather on power interruptions.

3. Data and Feature Description

Our database of Emergency Control System (ECS) tickets from Con Edison includes over a decade of trouble tickets for over thirty trouble types that represent events of interest. From the database, we compile triples $(s, t, e) \in \mathcal{S} \times \mathcal{T} \times \{0, 1\} = \mathcal{D}$, where s is the structure identifier, t is the date by month and e is a boolean value to indicate whether a structure s has a serious event during t . For example, triple (97429, 2001.8, 1) means structure “97429” had

a serious event in August, 2001. ECS tickets are assigned trouble types. We developed a machine-learned classifier to determine whether an event is serious, based on the ticket trouble type, language in the ticket, and structured data associated with the ticket.³ The experiments here use ECS tickets from 2000.1 to 2010.12 that refer to 46,729 secondary structures in Manhattan. This gives $46279 \times 11 \times 12 = 6,168,228$ triples.

Underground structures are not discrete entities. They are underground rooms that cables pass through, and that provide engineers with access to cable. Cables burn out and are replaced. To accommodate increased loads, additional cable can be added. Over time, a structure can become packed with cable, which is a strong but not sufficient predictor of serious events. In our previous work, we used four classes of features to model structure vulnerability: structure (structure type, location and identifier), cable (e.g., function–meaning main or service; phase or neutral; amount of cable; insulation material; year of installation), inspection, and electrical event features. At the time of this study, we had delivered a ranking model to predict 2011 vulnerability derived from a preliminary phase of feature selection that yielded 24 features. For convenience, we use the same 24 structure features here.

The weather features come from NYC open data and the National Climatic Data Center (NCDC). We derived 51 features to model monthly weather conditions, predominantly temperature and precipitation features based on domain expert knowledge. Con Edison engineers have suggested that structures are more vulnerable to events when rainwater or salt water (from melting ice and snow) leaks into them. Events also tend to occur during long periods of intense heat, which increases use of air conditioning, and therefore load on the system.

4. Model Description

The main objectives of the model presented here are interpretability and generality. We want to understand which aspects of weather are most stressful to the grid, and which properties of structures lead to increased incidence of serious events in certain years (e.g., see 2003 in Figure 1). A flat linear model cannot capture the *dependency* between parameters. We also want to understand the variation across years shown in Figure 1. Here we define a model that captures the dependency between structure and weather features. Our experiments contrast this model with a baseline logistic regression that uses the same features. We make the simplest possible non-trivial characterization of the weather, namely that a year is either good ($b = 0$) or bad ($b = 1$). Define the probability of structure s having a serious event ($e = 1$) or not ($e = 0$) at time frame t as $P(e|s, t)$:

$$P(e|s, t) = \sum_{b=0}^1 P(e, b|s, t) = \sum_{b=0}^1 P(e|s, b, t)P(b|t). \quad (1)$$

The first term defines the probability that a structure s has a serious event in a good or bad time frame. The underlying assumption is that whether a structure has a serious event can be predicted not only by its physical properties (location, connectivity, density of cables), but also by the severity of temporal conditions (b). Then $P(b|t)$ defines the probability that t is “bad.” We use log-linear models for the weather features and structure features. Define our model parameter $\theta = \{\mathbf{W}^+, \mathbf{W}^-, \mathbf{V}, \mathbf{bias}, Int, Int_+, Int_-\}$ as:

$$\begin{aligned} P(e = 1|s, t, b = 1) &= \Phi^+(s, t) = \frac{\exp(\mathbf{W}_+' \mathbf{F}(s, t) + Int_+)}{1 + \exp(\mathbf{W}_+' \mathbf{F}(s, t) + Int_+)} \\ P(e = 1|s, t, b = 0) &= \Phi^-(s, t) = \frac{\exp(\mathbf{W}_-' \mathbf{F}(s, t) + Int_-)}{1 + \exp(\mathbf{W}_-' \mathbf{F}(s, t) + Int_-)} \\ P(b = 1|t) &= \Phi(t) = \frac{\exp(\mathbf{V}' \mathbf{F}(t) + bias(t) + Int)}{1 + \exp(\mathbf{V}' \mathbf{F}(t) + bias(t) + Int)} \end{aligned} \quad (2)$$

where $\mathbf{F}(t) = [f_1(t), f_2(t), \dots]$ is the feature vector of weather on time t and $\mathbf{V} = [v_1, v_2, \dots]$ is the vector of the corresponding coefficients. From the definition, we can see that the lengths of \mathbf{W}_+ and \mathbf{W}_- correspond to the number of structure features. The length of \mathbf{V} is the number of weather features. The **bias** is the month-specific weight. In practice, we append the “1” indicator and month indicator to the input feature vectors and calculate *bias*, *Int*, *Int+* and *Int-* together with the regular coefficients. Then the probability $P(e, b|s, t)$ is from two binomial distributions:

$$P(e, b|s, t) = P(e|s, t, b)P(b|t) = \Phi^b(s, t)^e (1 - \Phi^b(s, t))^{1-e} \Phi(t)^b (1 - \Phi(t))^{1-b}. \quad (3)$$

4.1. The Expectation-Maximization Algorithm for Fitting our Model

We maximize our Q function as shown in Equation 4. The formulas here are presented without regularization terms for simplicity. In our experiment, to assist with feature selection, we use L1 (Lasso) regularization to control the parameters. The terms τ will be explained in **E-step**.

$$Q(\theta) = \sum_{(s,t,e) \in \mathcal{D}} \sum_{b=0}^1 \tau_{st}^{be} \left(e \log \Phi^b(s,t) + (1-e) \log(1 - \Phi^b(s,t)) + b \log \Phi(t) + (1-b) \log(1 - \Phi(t)) \right) \quad (4)$$

The \mathcal{D} here is defined in Section 3.

E-step: The prior distribution $P(b|s, t, e)$ is defined by:

$$\tau_{st}^{11} = P(b=1|e=1, s, t) = \frac{\Phi^+(s,t)\Phi(t)}{\Phi^+(s,t)\Phi(t) + \Phi^-(s,t)(1-\Phi(t))} \quad (5)$$

$$\tau_{st}^{01} = P(b=0|e=1, s, t) = \frac{\Phi^-(s,t)(1-\Phi(t))}{\Phi^+(s,t)\Phi(t) + \Phi^-(s,t)(1-\Phi(t))}$$

The other two priors can be computed from the above priors: $\tau_{st}^{10} = 1 - \tau_{st}^{11}$, $\tau_{st}^{00} = 1 - \tau_{st}^{01}$

M-step: For parameter \mathbf{V} , as there is no closed form solution for the equation $\frac{\partial Q}{\partial v_i} = 0$, we use gradient ascent as an alternative approach. The derivative with respect to v_i is:

$$\frac{\partial Q}{\partial v_i} = \sum_t f_i(t) \left(\sum_{s \in t^+} \tau_{st}^{11} + \sum_{s \in t^-} \tau_{st}^{10} - N_s \Phi(t) \right) \quad (6)$$

where $(s, t) \in E^+ \Leftrightarrow (s, t, 1) \in \mathcal{D}$. N_s is the total number of structures. As $\sum_{s \in t^+} \tau_{st}^{11} + \sum_{s \in t^-} \tau_{st}^{10} - N_s \Phi(t)$ can be computed before M-step, the computational cost for each iteration is $O(\text{len}(\mathbf{V}))$. Similarly, the update rule for structure parameters is:

$$\frac{\partial Q}{\partial w_i^+} = \sum_s \left(\sum_{t \in s^+} \tau_{st}^{11} (1 - \Phi^+(s,t)) f_i(s,t) - \sum_{t \in s^-} \tau_{st}^{10} \Phi^+(s,t) f_i(s,t) \right) \quad (7)$$

$$\frac{\partial Q}{\partial w_i^-} = \sum_s \left(\sum_{t \in s^+} \tau_{st}^{01} (1 - \Phi^-(s,t)) f_i(s,t) - \sum_{t \in s^-} \tau_{st}^{00} \Phi^-(s,t) f_i(s,t) \right)$$

where $t \in s^+ \Leftrightarrow (s, t, 1) \in \mathcal{D}$.

4.2. Prediction

A prediction in our problem consists of the list of structures ranked by their vulnerability in a given year y . The vulnerability score of structure s in time t in our problem is given by $P(e=1|s, t)$. Given a ranked list for year y , the position of the item with score v is defined by $Pos_y(v)$. In our problem, the order of structure s in the list is $Order_y(s)$. Hence we have:

$$\begin{aligned} Order_y(s) &= Pos_y(P(e=1|s, y)) = Pos_y \left(\sum_{m=jan}^{dec} P(e=1, m|s, y) \right) = Pos_y \left(\sum_{m=jan}^{dec} P(e=1|s, m, y) P(m|y) \right) \\ &= Pos_y \left(\sum_{m=jan}^{dec} P(e=1|s, m, y) \right) \end{aligned} \quad (8)$$

The justification for the last equation is that $P(m|y)$ is a unified distribution (1/12) that does not affect the order of a structure. As the result, we can generate a by-year structure ranking based on the sum of the by-month structure vulnerability.

Table 1. General evaluation results on 2010. The best value (or values, if tied) in each condition is in boldface.

Evaluation	Structure	Structure&Month	Structure&Month&Weather	EM-loglinear
Log-likelihood	-6420.00	-6196.28	-6061.64	-6054.05
Entropy	966.05	1048.25	1032.12	1048.00
AUC	0.5973	0.5980	0.6001	0.6026
P@5%	0.0974	0.0999	0.0974	0.0999
P@10%	0.1608	0.1583	0.1644	0.1742
P@20%	0.2960	0.2984	0.3033	0.3033

5. Experiments

We trained two models on 2000–2008, using 2009 as a development (validation) set and 2010 as the test set. We produced three baseline logistic regression models, each with a different feature set. The first uses only structure features, the second adds a month indicator, which captures the inherent temporal bias in the domain for structures to have bad events in winter and summer months. The third adds the weather features. Our EM model uses the same set of features as the last baseline. Unsurprisingly, the log-likelihood of the logistic regression models increases with additional features. The EM model with three embedded log-linear models has marginally better log-likelihood, so the increase in interpretability we discuss below is not at the expense of model fit.

Table 1 shows the AUC scores for each model. We also calculate precision at the top 5%, 10% and 20%. Finally, we calculate the entropy of each model to compare against the uniform distribution, whose entropy is 947.48.

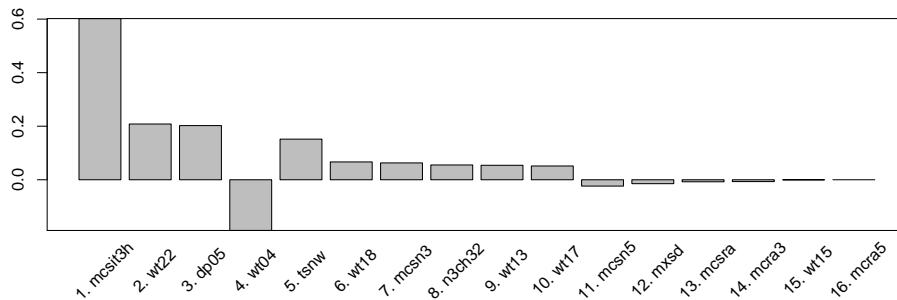


Fig. 2. Non-Zero coefficients of weather features ordered by absolute value for EM-Loglinear

6. Discussion

The benefit of the EM-loglinear model is its interpretability, which stems from having distinct representations for weather (V), structure vulnerability independent of the weather (W^-), and weather-induced structure vulnerability (W^+). Note that in principle, a flat logistic regression model could use product features such as " $f_1=10$ and weather = bad" to produce an equally interpretable result. However, without the EM estimation that treats weather severity as a hidden variable, we have no way to determine the values to assign to the product features. Also, features such as " $f_1=10$ and weather = bad" and " $f_1=10$ and weather = not bad" will be collinear if " f_1 " has nothing to do with the weather. For the EM model, we need consider collinearity only within structure features or within weather features. A few structure features had opposite signs for the two models (W^- and W^+), a possible sign of collinearity. When we increased the regularization parameter, however, we found the same relative trend for these coefficients, which eliminates the collinearity concern. In this section, we discuss interpretation of the dependencies.

6.1. What features define weather associated with an increase in serious events?

In contrast to the linear regression, the EM-loglinear model can directly estimate weather severity based on the likelihood of the data. Figure 2 shows the following weather features to be important:

1. **mcsit3h**: Number of consecutive days (≥ 3) where the high temperature is around freezing ($>5C$ and $<5C$) (\cdot).
2. **wt22**: Number of days with ice fog or freezing fog; the weather is wet but not cold.
3. **dp05**: Number of days at least 0.5 inches of precipitation
4. **wt04**: Number of days with ice pellets, sleet, snow pellets, or small hail. This is a negative feature. A possible explanation is that the temperature is low enough to prevent ice from melting and entering the structures.
5. **tsnw**: Total snow fall, which can enter the structure if it melts.
6. **wt18**: Number of days with snow, snow pellets, snow grains, or ice crystals. Like **10** below, this corresponds to cold and wet weather, but the precipitation includes ice.
7. **mcsn3**: Number of consecutive days (≥ 3) of snow. With continuing snow, the city continues to spread salt in the streets. The combination of precipitation and salt causes problems in structures.
8. **n3ch32**: Number of consecutive days (≥ 3) of high temperature ($>32C$). A long period of high temperature can correspond to increased load on structures due to constant use of air conditioning.
9. **wt13**: Number of days with mist.
10. **wt17**: Number of days with freezing rain.

Most of the features related to bad weather pertain to winter weather near but not below freezing, and to precipitation. This accords well with reports from Con Edison engineers that the worst conditions are when there is precipitation and water enters the structures, and when snow or ice mixed with salt melts into the structures. If the temperature is well below freezing, then ice and snow do not melt, and the structures are unaffected.

The flat linear regression model can incorporate exactly the same weather features. Their relative importance, however, cannot be inferred from the coefficients. Because the model is trained and regularized with structure features and weather features together, the response does not directly represent weather severity.

6.2. What structure features increase the vulnerability given inclement weather?

In our past models, features for the number of cable conductors (individual cables) or cable sets (phases and neutrals within a single bundle) show that more cables lead to greater vulnerability. The base cause of many events is insulation breakdown, so these features are predictive because they represent number of locations for insulation

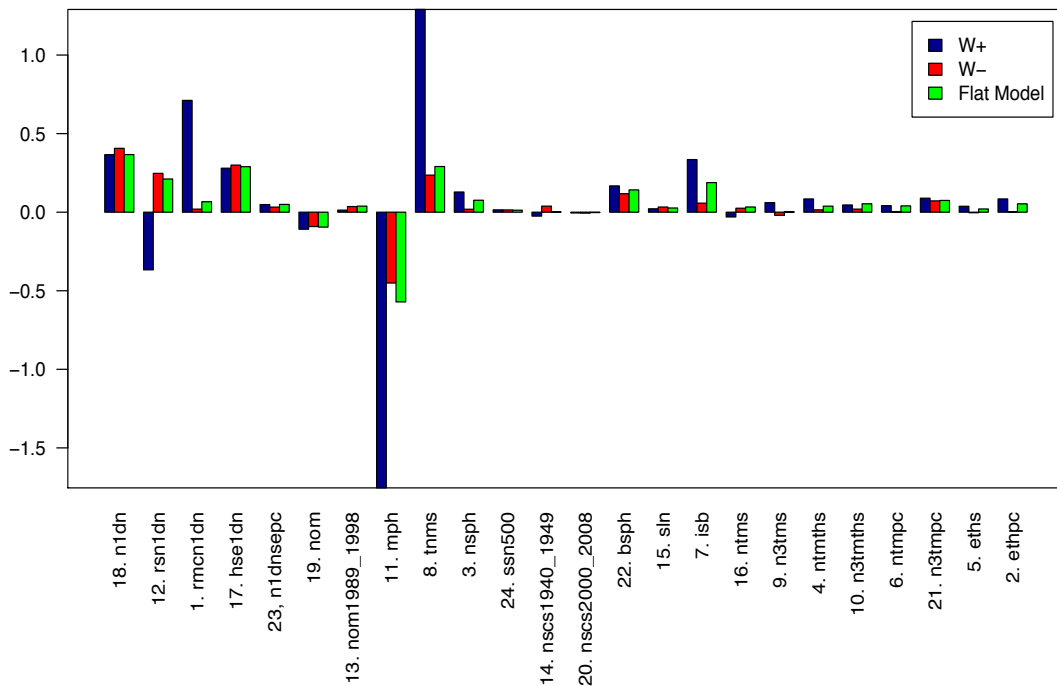


Fig. 3. Coefficients of Structure Features in the Three Models

Table 2. Ranked list of structure feature by W+ and W-

Structure Feature	Order(W-)	Order(W+)	Order(W-)-Order(W+)
1. rmcn1dn. Ratio of the number of main conductors to one-degree neighbors	16	3	13
2. ethpc. Has been a trouble hole for non-serious events	24	12	12
3. nsph. Number of service phase cables	18	9	9
4. ntmths. Number of times mentioned as the trouble hole of serious events	19	13	6
5. eths. Has been a trouble hole for serious events	23	18	5
6. ntmpc. Number of times mentioned in non-serious events	22	17	5
7. isb. The structure is a service box	9	6	3
8. tnms. Number of main cable sets	5	2	3
9. n3tms. Number of times mentioned in serious events in the past 3 years	15	14	1
10. n3tmths. Number of times mentioned as the trouble hole of serious events in the past 3 years	17	16	1
11. mph. Number of main phase cables	1	1	0
12. rsn1dn. Ratio of number of sets to one-degree neighbors	4	4	0
13. nom1989_1998. Number of main cable sets entered from 1989 to 1998	11	23	-12
14. nscs1940_1949. Number of service cable sets entered from 1940 to 1949	10	20	-10
15. sln. Street lights neutral	12	21	-9
16. ntms. Number of times mentioned as serious	14	19	-5
17. hse1dn. Number of serious events on one-degree neighbors	3	7	-4
18. n1dn. Count of one-degree neighbors	2	5	-3
19. nom. Total number of (past and present) open mains	7	10	-3
20. nscs2000_2008. Number of service cable sets entered from 2000 to 2008	21	24	-3
21. n3tmpc. Number of times mentioned as precursor in the past 3 years	8	11	-3
22. bsph. Whether it has service phase cable	6	8	-2
23. n1dnsepc. One-degree neighbor has serious event or precursor event	13	15	-2
24. ssn500. The neutral service cable is size 500 Kcmll	20	22	-2

breakdown. Figure 3 shows the feature weights of W- (red), W+ (dark blue) and the baseline model (green). Table 2 describes each feature. The green bars in Figure 3 (the flat model) often fall between the coefficients for W+ and W-, but not always. Features sometimes have high coefficients for all models (17 and 18 in Figure 3), and others are important for weather-induced vulnerability (1, 7 and 8) or have strongly opposing influence for W+ and W- (12).

11. mph: The number of main phase (non-neutral) mains conductors is negative in both W+ and W-, with much greater absolute value for W+. The negative correlation is unusual for cable density features. A testable interpretation is that structures where relatively more of the cables are main phase are more likely to be *critical manholes*, a group of structures that Con Edison prioritizes for maintenance and repair, due to their importance in the network.

7. isb and 8. tnms: These two features have high coefficients in both models, but much higher in W+. **7** is a boolean indicator for service boxes, structures that have lower overall cable capacity on average, and that are more likely to have service cables directly to customers. **8** is the number of cable sets (bundles; see above) of mains cables. An interpretation of these two features combined with **11** would be that structures with many main phase and no service cables are less likely to have serious events (critical manholes), while structures that are not critical manholes are more vulnerable if they are service boxes, or if they have many sets of mains.

1. rmcn1dn: This feature, ratio of main conductors per one-degree neighbor, has a high positive coefficient in W+ and a relatively low one in W-. A structure's one-degree neighbors are the structures it connects to directly by cable, with no intervening structures. Most structures have only a few one-degree neighbors (2 to 3), but some have many. High values indicate many cable conductors per immediate neighbor, and therefore, per duct. As mentioned above, cable density features are generally predictive, which we attribute to more locations where insulation can break down. That normalizing by the number of immediate neighbors is highly predictive only for W+ suggests an interpretation that could be tested. Stressful weather conditions often lead to water or salt water seeping into the structure. It is possible that water in the structure is more likely to cause a serious event the more opportunity it has to come into direct contact with exposed conductor. This is perhaps more likely in a densely packed duct.

12. rsn1dn: Where **1** normalizes the number of conductors by one-degree neighbors, **12** normalizes the number of sets (bundled main and neutral cables) by one-degree neighbors. Where **1** had positive coefficients in both models, **12** has opposite values: a positive coefficient for W- and a negative one for W+. Most often, one or two sets of

cable are sufficient to connect any pair of immediate neighbors, but some structures are connected by many sets. This feature indicates that with relatively more sets per neighbor, a structure is more likely to have a serious event in good weather, and less likely in bad weather. One of our original motivations for the dependency model presented here was to account for differences in performance of our original approach for years with many versus few events. That this feature has opposite influence in the two models shows the need for separate models of baseline versus weather-enhanced vulnerability. We suggest that baseline vulnerability represents factors that lead to insulation breakdown, which happens slowly over time, and that more sets per neighbor may produce conditions in the structure that have a steady impact on this process. Conversely, more sets per neighbor corresponds to more ducts per neighbor, which may counteract the impact of water seeping into the structure, which otherwise has a short term impact on serious events: the water may have more places to go, with a lower likelihood of coming into contact with exposed conductor.

Table 2 lists the 24 structure features, ordered by the difference in rank of the coefficient between the baseline structure model (W^-) and the weather-enhanced one (W^+). Features that capture cable or insulation materials, such as the year of installation of cables (e.g., **14. nscs1940.1949**), and the grid configuration, such as count of one-degree neighbors (**18. n1dn**), have higher weights under ordinary weather conditions than under bad weather conditions. Features that are relatively higher when the weather is bad include cable density features, such as the ones discussed above, and features pertaining to event history, such as **2. ethpc**.

7. Conclusion

The modeling approach presented here separates the two phenomena of weather and structures, and models their dependencies. This yields greater interpretability of the impact of weather versus structure features. It confirms and adds detail to the intuition from Con Edison engineers that the winter weather conditions that stress the grid consist of near-freezing temperatures combined with precipitation. Further, the two models for baseline structure vulnerability and weather-induced vulnerability help account for the marked differences in vulnerability from year to year. The results indicate that a structure's baseline vulnerability has more to do with the time frame when cables were installed (a proxy for the kinds of conductor and insulation materials). A structure's increased vulnerability during bad weather is associated with features representing its event history (the red curve in Figure 1) and how densely packed the structure is with cable, as in our earlier models, but more subtly, how the cable is distributed, which was not evident in our earlier models. Future work will focus on feature selection to improve prediction accuracy across years.

References

1. Rudin, C.. The P-Norm Push: A simple convex ranking algorithm that concentrates at the top of the list. *Journal of Machine Learning Research* 2009;**10**:2233–2271.
2. Rudin, C., Passonneau, R., Radeva, A., Dutta, H., Jerome, S., Isaac, D.. A process for predicting manhole events in Manhattan. *Machine Learning* 2010;**80**:1–31.
3. Xie, B., Passonneau, R., Dutta, H., Miaw, J.Y., Radeva, A., Tomar, A., et al. Progressive clustering with learned seeds: An event categorization system for power grid. In: *24th International Conference on Software Engineering and Knowledge Engineering (SEKE 2012)*. Redwood City, CA; 2012, p. 100–105.
4. Passonneau, R., Rudin, C., Radeva, A., Liu, Z.A.. Reducing noise in labels and features for a real world dataset: Application of NLP corpus annotation method. In: *Proceedings of the 10th International Conference on Computational Linguistics and Intelligent Text Processing (CICLing)*. 2009, p. 86–97.
5. Geurts, P., Wehenkel, L.. Early prediction of electric power system blackouts by temporal machine learning. In: *Proc. of ICML-AAA'I'98 Workshop on AI Approaches*. AAAI Press; 1998, p. 21–28.
6. Hatziairyriou, N.. Machine learning applications to power systems. In: Paliouras, G., Karkaletsis, V., Spyropoulos, C.D., editors. *Machine Learning and its Applications*. 2001, p. 308–317.
7. Anderson, R.N., Boulanger, A., Powell, W.B., Scott, W.. Adaptive stochastic control for the smart grid. *Proceedings of the IEEE* 2011; **99**(6):1098–1115.
8. Gross, P., Boulanger, A., Arias, M., Waltz, D.L., Long, P.M., Lawson, C., et al. Predicting electricity distribution feeder failures using machine learning susceptibility analysis. In: *AAAI*. AAAI Press; 2006, p. 1705–1711.
9. Dhiman, G., Rosing, T.S.. Dynamic power management using machine learning. In: *Proceedings of the 2006 IEEE/ACM International Conference on Computer-aided Design*. ACM; 2006, p. 747–754.
10. Saad, W., Han, Z., Poor, H.V., Basar, T.. Game-theoretic methods for the smart grid: An overview of microgrid systems, demand-side management, and smart grid communications. *Signal Processing Magazine, IEEE* 2012;**29**(5):86–105.
11. Sharma, N., Sharma, P., Irwin, D., Shenoy, P.. Predicting solar generation from weather forecasts using machine learning. In: *Proceedings of the Second IEEE International Conference on Smart Grid Communications (SmartGridComm)*. 2011, p. 528–533.